

Microwave-Accelerated Metal-Enhanced Fluorescence: Platform Technology for Ultrafast and Ultrabright Assays

Kadir Aslan[†] and Chris D. Geddes^{*,†,‡}

Institute of Fluorescence, Laboratory for Advanced Medical Plasmonics, Medical Biotechnology Center, University of Maryland Biotechnology Institute, 725 West Lombard Street, Baltimore, Maryland 21201, and Center for Fluorescence Spectroscopy, Medical Biotechnology Center, University of Maryland School of Medicine, 725 West Lombard Street, Baltimore, Maryland 21201

We describe an exciting assay platform technology that promises to fundamentally address two underlying physical constraints of modern assays and immunoassays, namely, assay sensitivity and rapidity. By combining the use of metal-enhanced fluorescence with low-power microwave heating, we can indeed significantly increase the sensitivity of surface assays as well as >95 % kinetically complete the assay within a few seconds. Subsequently, this new technology promises to fundamentally change the way we currently employ immunoassays in clinical medicine. This new model platform system can be potentially applied to many other important assays, such as to the clinical assessment of myoglobin, where both assay speed and sensitivity is paramount for the assessment and treatment of acute myocardial infarction. To demonstrate the utility of microwave-accelerated metal-enhanced fluorescence (MAMEF), we show that a simple protein-based assay system can be optically amplified ~10-fold by using silver nanostructures, while being kinetically complete in less than 20 s. This new platform approach is subsequently over 10-fold more sensitive and ~90 times faster than a control assay that operates both at room temperature and without the use of metal-enhanced fluorescence. Finally, we show that low-power heating by microwaves in our model system does not denature proteins, as evidenced by no protein structural changes, probed by fluorescence resonance energy transfer.

Immunoassays are widely used for the detection and determination of a wide variety of proteins, peptides, and small molecules.^{1–8} While there exists a large diverse family of immu-

noassays today, the basic principles are mostly the same.^{1–8} These typically use antigen–antibody binding for analyte recognition and mostly fluorescence-based readout for signal transduction. Fluorescent-based immunoassays are available in many forms, such as time-resolved immunoassays,^{9–13} energy-transfer immunoassays,^{14–16} and fluorescence polarization immunoassays.^{17,18}

The antigen–antibody recognition step is most often kinetically very slow, requiring long incubation times, very few assays subsequently being complete less than 10 min.^{1–8} In addition, the sensitivity of fluorescence-based immunoassays is mostly governed by the quantum yield of the tagging fluorophore and the efficiency and sensitivity of the detection system.^{1–8} These two physical constraints underpin both the rapidity and sensitivity of current immunoassays.^{1–8}

In this regard, we have combined the use of metal-enhanced fluorescence (MEF),^{19–21} a relatively new technology that can dramatically increase the quantum yield and photostability of weakly fluorescing species,^{19–21} with the use of low-power micro-

* To whom correspondence should be addressed. E-mail: geddes@umbi.umd.edu.

[†] University of Maryland Biotechnology Institute.

[‡] University of Maryland School of Medicine.

- (1) Bange A.; Halsall, H. B.; Heineman, W. R. *Biosens. Bioelectron.* **2005**, *20* (12), 2488–2503.
- (2) Hemmilam L. A. *Applications of Fluorescence in Immunoassays*; John Wiley and Sons: New York, 1992.
- (3) Van Dyke, K.; Van Dyke, R., Eds. *Luminescence Immunoassay and Molecular Applications*; CRC Press: Boca Raton, FL, 1990.
- (4) Ozinkas, A. J. Principles of Fluorescence Immunoassay, In *Topics in Fluorescence Spectroscopy*; Lakowicz, J. R., Ed.; Plenum Press: New York, 1994; Vol. 4.

- (5) Gosling, J. P. *Clin. Chem.* **1990**, *36*, 1408–1427.
- (6) Davidson, R. S.; Hilchenbach, M. M. *Photochem. Photobiol.* **1990**, *52*, 431–438.
- (7) Vo-Dinh, T.; Sepaniak, M. J.; Griffin, G. D.; Alarie, J. P. *Immunoassays* **1993**, *3*, 85–92.
- (8) Schweitzer, B.; Kingsmore, S. F. *Curr. Opin. Biotechnol.* **2002**, *13*, 14–19.
- (9) Lovgren, T.; Hemmila, I.; Petterson, K.; Halonen, P. Time-Resolved Fluorometry in Immunoassay. In *Alternative Immunoassays*; Collins, W. P., Ed.; John Wiley and Sons: New York, 1985.
- (10) Diamendis, E. P. *Clin. Chem.* **1988**, *21*, 139–150.
- (11) Lovgren, T.; Petterson, K. Time-Resolved Fluoroimmunoassay: Advantages and Limitations. In *Luminescence Immunoassay and Molecular Applications*; CRC Press: Boca Raton, FL, 1990.
- (12) Khosravi, M.; Diamendis, E. P. *Clin. Chem.* **1987**, *33*, 1993–1999.
- (13) Soini, E. Pulsed light, Time-Resolved Fluorometric Immunoassay. In *Monoclonal Antibodies and New Trends in Immunoassays*; Bizollon, C. A., Ed.; Elsevier Science Publishers: New York, 1984.
- (14) Ullman, E. F.; Schwarzbach, M.; Rubenstein K. E. *J. Biol. Chem.* **1976**, *251*, 4172–4178.
- (15) Ozinkas, A. J.; Malak, H.; Jaoshi, J.; Szmactinski, H.; Britz, J.; Thompson, R. B. Koen, P. A. Lakowicz, J. R. *Anal. Biochem.* **1993**, *213*, 264–270.
- (16) Lakowicz, J. R.; Ozinkas, A. J.; Thompson, R. B. *Sens. Actuators* **1993**, *12*, 65–70.
- (17) Dandliker, W. B.; Saussure, V. A. *Immunochemistry* **1970**, *7*, 799–828.
- (18) Spencer, R. D.; Toledo, F. B.; Williams, B. T.; Yoss, N. L. *Clin. Chem.* **1973**, *19*, 838–844.
- (19) Aslan, K.; Gryczynski I.; Malicka J.; Matveeva E.; Lakowicz, J. R.; Geddes, C. D. *Curr. Opin. Biotechnol.*, **2005**, *16*(1), 55–62.
- (20) Geddes, C. D.; Aslan, K.; Gryczynski, I.; Malicka, J.; Lakowicz, J. R. In *Annual Reviews in Fluorescence 2004*; Geddes, C. D., Lakowicz, J. R., Eds; Kluwer Academic/Plenum Publishers: New York, 2004; pp 365–401.

waves, which can kinetically accelerate assays. The unique combination of both technologies serves to demonstrate in this paper that the current bottlenecks of immunoassay sensitivity and rapidity can be alleviated.

In the last five or so years, our laboratories have demonstrated many applications of metal-enhanced fluorescence,^{19–21} where the origins of MEF can be traced back to several groups working in this area.^{22,23} These applications have included the increased detectability and photostability of fluorophores,^{24–26} improved DNA detection,²⁷ release of self-quenched fluorescence of over-labeled proteins,²⁸ and application of metallic surfaces to amplified wavelength-ratiometric sensing,²⁹ to name but just a very few. In addition, we have developed many surfaces for metal-enhanced fluorescence,^{30–34} such as those composed of silver islands,³⁰ silver colloids,³¹ silver nanotriangles,³² silver nanorods,³³ and even fractal-like silvered surfaces.³⁴ Several modes of silver deposition have also been developed, such as silver deposition by light³⁵ and electrochemically³⁶ on glass²⁵ plastics³⁷ and even electrodes.³⁸

In all of these applications of MEF it has been shown that the enhanced fluorescence signals (quantum yields, Q_m) of fluorophores in proximity (<10 nm) to metallic nanostructures could be well described by the following equations:

$$Q_m = (\Gamma + \Gamma_m) / (\Gamma + \Gamma_m + k_{nr}) \quad (1)$$

where Γ is the unmodified radiative decay rate, Γ_m is the metal-modified radiative decay rate, and k_{nr} are the nonradiative rates. Similarly, the metal-modified lifetime, τ_m , of a fluorophore is decreased by an increased radiative decay rate:

$$\tau_m = 1 / (\Gamma + \Gamma_m + k_{nr}) \quad (2)$$

These equations have resulted in most unusual predictions for

- (21) Geddes, C. D.; Aslan, K.; Gryczynski, I.; Malicka, J.; and Lakowicz, J. R. In *Topics in Fluorescence Spectroscopy*; Geddes, C. D., Lakowicz, J. R., Eds.; Kluwer Academic/Plenum Publishers: New York, 2005; pp 401–448.
- (22) Weitz, D. A.; Garoff, S.; Hanson, C. D.; Gramila, T. J.; Gersten, J. I., *Opt. Lett.* **1982**, *7* (2), 89–91.
- (23) Wokaun, A.; Lutz, H.-P.; King, A. P.; Wild, U. P.; Ernst, R. R., *J. Chem. Phys.* **1983**, *79* (1), 509–513.
- (24) Lakowicz, J. R. *Anal. Biochem.* **2001**, *298*, 1–24.
- (25) Lakowicz, J. R.; Shen, Y.; D'Auria, S.; Malicka, J.; Fang, J.; Gryczynski, Z.; Gryczynski, I. *Anal. Biochem.* **2002**, *301*, 261–277.
- (26) Lakowicz, J. R.; Shen, Y.; Gryczynski, Z.; D'Auria, S.; Gryczynski, I. *Biochem. Biophys. Res. Commun.* **2001**, *286*, 875–879.
- (27) Malicka, J.; Gryczynski, I.; Lakowicz, J. R. *Biochem. Biophys. Res. Commun.* **2003**, *306*, 213–218.
- (28) Lakowicz, J. R.; Malicka, J.; D'Auria, S.; Gryczynski, I. *Anal. Biochem.* **2003**, *320*, 13–20.
- (29) Aslan, K.; Lakowicz, J. R.; Szmajcinski, H.; Geddes, C. D. *J. Fluoresc.* **2005**, *15* (1), 37–40.
- (30) Malicka, J.; Gryczynski, I.; Geddes, C. D.; Lakowicz, J. R. *J. Biomed. Opt.* **2003**, *8* (3), 472–478.
- (31) Geddes, C. D.; Cao, H.; Gryczynski, I.; Gryczynski, Z.; Fang, J.; Lakowicz, J. R. *J. Phys. Chem. A* **2003**, *107* (18), 3443.
- (32) Aslan, K.; Lakowicz, J. R.; Geddes, C. D. *J. Phys. Chem. B* **2005**, *109*, 6247–6251.
- (33) Aslan, K.; Leonenko, Z.; Lakowicz, J. R.; Geddes, C. D.; *J. Phys. Chem. B* **2005**, *109* (8), 3157–3162.
- (34) Parfenov, A.; Gryczynski, I.; Malicka, J.; Geddes, C. D.; Lakowicz, J. R. *J. Phys. Chem. B* **2003**, *107* (34), 8829–8833.
- (35) Geddes, C. D.; Parfenov, A.; Lakowicz, J. R. *Appl. Spectrosc.* **2003**, *57* (5), 526–531.
- (36) Geddes, C. D.; Parfenov, A.; Roll, D.; Fang, J.; Lakowicz, J. R. *Langmuir* **2003**, *19* (15), 6236–6241.

fluorophore–metal combinations, and it is these predictions and observations that are currently finding profound implications and applications in fluorescence-based nanotechnology.^{19–21,24,39} Given that fluorescence has become the dominant tool in biotechnology today, then metal-enhanced^{19–21,24,39} and plasmon-coupled fluorescence^{40,41} promises to change the way we both use and think about fluorescence.⁴² From eqs 1 and 2, we can see that as the value of Γ_m increases, the quantum yield Q_m increases, while the lifetime, τ_m , decreases. This is contrary to most observations in fluorescence⁴² where the free-space quantum yield, Q_0 , and lifetime, τ_0 , usually change in unison⁴² as described by the well-known equations:⁴²

$$Q_0 = \Gamma / (\Gamma + k_{nr}) \quad (3)$$

$$\tau_0 = 1 / (\Gamma + k_{nr}) \quad (4)$$

In addition, one major criterion for choosing fluorophores in current immunoassays has been a high quantum yield. This can lead to a high background from either unlabeled fluorophores or a high fluorescence background from nonspecific assay absorption. However, metal-enhanced fluorescence is ideally suited in this regard, in that low quantum yield fluorophores are more favorable,^{2,25,39} the fluorescence enhancement factor in the presence of silver nanostructures given by $1/Q_0$ where Q_0 is the free-space²⁴ quantum yield in the absence of metal. Subsequently, MEF, when applied to immunoassays, promises to yield ultra-bright assays, with a much higher signal/noise ratio as compared to identical assays not employing the MEF phenomenon. In this regard, our laboratory has recently published the metal-enhanced fluorescence detection of myoglobin using evanescent-wave excitation, but in a total internal reflection fluorescence geometry.⁴³

In the past two decades, the use of microwave radiation has greatly increased in radar and communication systems,⁴⁴ for accelerating reactions in synthetic organic chemistry applications,^{45–47} in drug delivery,⁴⁸ assays,^{49–53} and biochemistry.^{54–56} The development of medical microwave-based devices for clinical diagnosis and therapy has also prompted widespread interest and

- (37) Aslan, K.; Badugu, R.; Lakowicz, J. R.; Geddes, C. D. *J. Fluoresc.* **2005**, *15* (2), 99–104.
- (38) Geddes, C. D.; Parfenov, A.; Roll, D.; Gryczynski, I.; Malicka, J.; Lakowicz, J. R. *Spectrochim. Acta, Part A* **2004**, *60* (8–9), 1977–1982.
- (39) Geddes, C. D.; Lakowicz, J. R. *J. Fluoresc.* **2002**, *12* (2), 121–129.
- (40) Geddes, C. D.; Gryczynski, I.; Malicka, J.; Gryczynski, Z.; Lakowicz, J. R. *Photonics Spectra* **38** (2), 92+ February 2004.
- (41) Lakowicz, J. R. *Anal. Biochem.* **2004**, *324* (2), 153–169.
- (42) Lakowicz, J. R. *Principles of Fluorescence Spectroscopy*; Kluwer: New York, 1999.
- (43) Matveeva, E.; Gryczynski, Z.; Malicka, J.; Gryczynski, I.; Lakowicz, J. R. *Anal. Biochem.* **2004**, *334* (2), 303–311.
- (44) Sridar, V. *Curr. Sci.* **1998**, *74* (5), 446–450.
- (45) Caddick, S. *Tetrahedron* **1995**, *51*, 10403–10432.
- (46) Sridar V. *Indian J. Chem., Sect. B: Org. Chem. Incl. Med. Chem.* **1997**, *36* (1), 86–87.
- (47) Varma, R. S. *Advances in Green Chemistry: Chemical Synthesis Using Microwave Irradiation*; Astrazeneca Research Foundation: Bangalore, India, 2002.
- (48) Lin, J. C.; Yuan, P. M. K.; Jung, D. T. *Bioelectrochem. Bioenerg.* **1998**, *47* (2), 259–264.
- (49) Akins, R. E.; Tuan, R. S. *Mol. Biotechnol.* **1995**, *4* (1), 17–24.
- (50) Rhodes, A.; Jasani, B.; Balaton, A. J.; Barnes, D. M.; Anderson, E.; Bobrow, L. G.; Miller, K. D. *Am. J. Clin. Pathol.* **2001**, *115* (1), 44–58.
- (51) Van Triest, B.; Loftus, B. M.; Pinedo, H. M.; Backus, H. H. J.; Schoenmakers, P.; Tellemann, F. J. *Histochem. Cytochem.* **2000**, *48* (6), 755–760.

stimulated much research on the mechanisms of interaction of low-power microwaves with living organisms.^{57–59}

Microwaves (~0.3–300 GHz) lie between the infrared and radio frequency electromagnetic radiations. It is widely thought that microwaves accelerate chemical and biochemical reactions by the heating effect,⁵⁷ where the heating essentially follows the principle of microwave dielectric loss.⁴⁴ Polar molecules absorb microwave radiation through dipole rotations and hence are heated, whereas nonpolar molecules do not absorb due to lower dielectric constants and thus are not heated.⁴⁴ The polar molecules align themselves with the external applied field. In the conventional microwave oven cavity employed in this work, the radiation frequency (2450 MHz) changes sign 2.45×10^9 times/s. Heating occurs due to the torsional effect as the polar molecules rotate back and forth, continually realigning with the changing field, the molecular rotations being slower than the changing electric field. The dielectric constant, the ability of a molecule to be polarized by an electric field, indicates the capacity of the medium to be microwave heated. Thus, solvents such as water, methanol, and dimethyl formamide are easily heated, whereas microwaves are effectively transparent to hexane, toluene, and diethyl ether.⁴⁴ For metals, the attenuation of microwave radiation arises from the creation of currents resulting from charge carriers being displaced by the electric field.⁶⁰ These conduction electrons are extremely mobile and unlike water molecules can be completely polarized in 10^{-18} s. In our microwave cavity, the time required for the applied electric field to be reversed is far longer than this, in fact by many orders of magnitude. If the metal particles are large, or form continuous strips, then large potential differences can result, which can produce dramatic discharges if they are large enough to break down the electric resistance of the medium separating the large metal particles. Interestingly, and most appropriate for our new assay platform described here, small metal particles do not generate sufficiently large potential differences for this “arcing” phenomenon to occur.⁶⁰ However, as we will discuss later, the charge carriers that are displaced by the electric field are subject to resistance in the medium in which they travel due to collisions with the lattice phonons.⁶⁰ This leads to ohmic heating of the metal nanoparticles in addition to the heating of any surface polar molecules. Intuitively, in our assay, this leads to localized heating around the silver nanostructures in addition to the solvent, rapidly accelerating assay kinetics. Further, the proximity of assay fluorophores, additionally leads to fluorophore radiative decay rate modifications^{24,39} and subsequent increase in fluorescence emission.^{24,39} Hence, metallic nanoparticles, fluorophores, and microwaves can be combined to yield kinetically accelerated and optically amplified immunoassays.

(52) Croppo, G. P.; Visvesvara, G. S.; Leitch, G. J.; Wallace, S.; Schwartz, D. A. *Arch. Pathol. Lab. Med.* **1998**, *122* (2), 182–186.

(53) Philippova T. M.; Novoselov, V. I.; Alekseev, S. I. *Bioelectromagnetics* **1994**, *15* (3), 183–192.

(54) Roy, I.; Gupta, M. N. *Curr. Sci.* **2003**, *85* (12), 1685–1693.

(55) Bismuto, E.; Mancinelli, F.; d'Ambrosio, G.; Massa, R. *Eur. Biophys. J.* **2003**, *32*, 628–634.

(56) Porcelli, M.; Cacciapuoti, G.; Fusco, S.; Massa, R.; d'Ambrosio, G.; Bertoldo, C.; DeRosa, M.; Zappia, V. *FEBS Lett.* **1997**, *402* (2–3), 102–106.

(57) Adam, D. *Nature* **2003**, *421*, 571–572.

(58) Whittaker, A. G.; Mingos, D. M. P. *J. Chem. Soc., Dalton Trans.* **1995**, *12*, 2073–2079.

(59) Kappe, C. O. *Curr. Opin. Chem. Biol.* **2002**, *6*, 314–320.

(60) Whittaker, A. G.; Mingos, D. M. P. *J. Chem. Soc., Dalton Trans.* **1993**, *16*, 2541–2543.

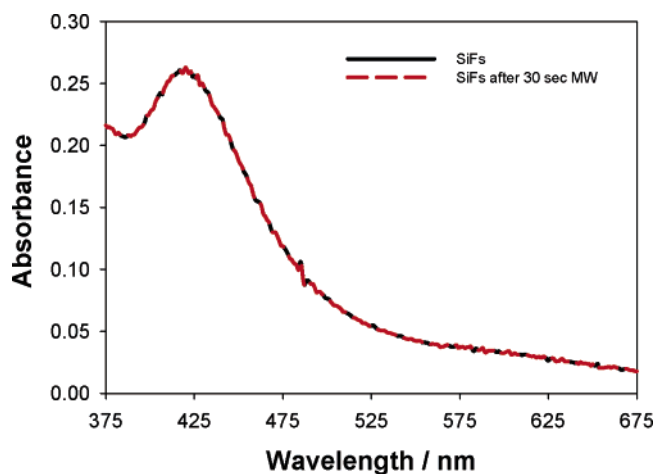


Figure 1. Silver island film (SiFs) plasmon absorption spectrum before and after exposure to low-power microwaves.

Finally, it is informative to comment on the use of microwaves in biochemical and biological systems. In the mid 1980s much controversy surrounded the use of microwaves due to the so-called “nonthermal” effects^{57–59} on biological systems, where some authors believed that the rates of reaction in many microwave-assisted reactions could not be explained by heating alone^{57–59} and have since questioned enzyme, DNA, and protein function and conformation after microwave exposure.^{57–59} On the other hand, some workers assert that there are no “nongeneral thermal effects”, and the so-called nonthermal effect is due to the superheating of solvents above their boiling points.⁵⁹ While this debate is likely to continue for some time, as it is difficult to experimentally prove a nonthermal effect, it is clearly evident that the use of low-power microwaves is rapidly growing, with many companies now selling microwave-based laboratory equipment and the publication of many articles a year embracing the technology. Interestingly, the “Technology Vision 2020” of the U.S. chemical industry believes that microwave heating will soon replace traditional heating in chemical and biochemical synthesis.^{61,62} To address the issue of nonthermal effects and possible protein conformational changes due to exposure to low-power microwave heating in our model assay system, we perform fluorescence resonance energy-transfer (FRET) experiments, where FRET is widely used to assess protein conformational changes.⁴² Our control experiments reveal no protein conformational changes for both fluorophore-labeled avidin and biotinylated bovine serum albumin (BSA), when exposed to <140-W, 2450-MHz microwaves.

RESULTS AND DISCUSSION

Figure 1 shows the plasmon absorption spectra of Silver Island films (SiFs), both before and after low-power microwave heating for 30 s. The cavity power was ~140 W, which is the same as utilized in the assays discussed later and is of a power similar to that used for immunostaining.^{63,64} As can be seen from Figure 1,

(61) Technology Vision 2020, The U.S. Chemical Industry, December 1996.

(62) Chen, S. T.; Sookheo, B.; Phutrahal, S.; Wang, K. T. Enzymes in Nonaqueous Solvents: Applications in Carbohydrate and Peptide Preparation. In *Enzymes in Nonaqueous Solvents: Methods and Protocols*; Vulfson E. N., Halliog P. J., Bolland, H. L., Eds.; Methods in Biotechnology 15; Humana Press: Totowa, NJ, 2001; pp 373–400.

(63) Micheva, K. D.; Holz, R. W.; Smith, S. J. *J. Cell Biol.* **2001**, *154*, 355–368.

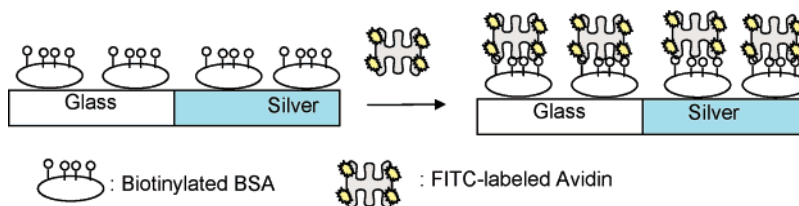


Figure 2. Model protein–fluorophore system used to demonstrate microwave-accelerated metal-enhanced fluorescence. Both glass and silvered surfaces are equally coated with biotinylated BSA, which creates a spacer layer for metal-enhanced fluorescence. Fluorescein-labeled avidin (FITC–avidin) rapidly binds to the surface with a room temperature reaction time of ~30 min.

the microwaves and heating had no effect on the surface plasmon absorption of the SiFs, indicating no structural or surface silver shape changes, where the surface plasmon absorption is well known to be characteristic of the shape of the nanoparticles,^{65,66} which is due to the mean free path oscillation of surface charges.^{65,66} Further, as briefly discussed in the introduction, no “sparking” was evident from the silvered surfaces, a known consequence of surface charge buildup and dissipation⁶⁰ for large nonwavelength-sized particles or continuous surfaces.⁶⁰

We additionally measured the structural morphology of the silvered surfaces using atomic force microscopy (AFM), data not shown. While it was somewhat difficult to probe that exact same area after microwave heating, very little, if no change in surface morphology was observed between the locations. In addition, we exposed the silvered surfaces, both wet and dry, to several hundred watts of microwave cavity power over many minutes. In all of these investigations, no evidence for surface structural changes was found by microwave heating, clearly demonstrating the compatibility of the nanostructured surfaces to microwave exposure and therefore heating. In this regard, several solution-based studies have recently reported the microwave-induced growth of nanostructures, although these reports involved only the initial growth of the particles in the presence of stabilizing surfactants^{67–71} and not the exposure of finalized structures as described here. In addition, our laboratories have recently reported the thermal annealing of SiFs and its subsequent effect on the MEF effect,⁷² where significant changes in the surface morphology only occur at very high temperatures, i.e., >200 °C.

To demonstrate the utility of our new platform assay approach we chose a model protein–fluorophore system, Figure 2, which equally coats half of a silvered glass microscope slide, the other side nonsilvered, acting as a control sample by which to compare the benefits of using the MEF phenomenon. The enhancement ratio $I_{\text{SiFs}}/I_{\text{glass}}$ (the benefit of using the MEF phenomenon) is the fluorescence intensity observed on the SiFs divided by the intensity on the nonsilvered glass substrate. Earlier studies by

our laboratories and others have shown that biotinylated BSA readily forms a monolayer on both silver and glass substrates.^{73–75} In addition, this protein system positions fluorophores at >4 nm from the surfaces, which is ideal for MEF, which both we and others have shown to be a through-space phenomenon.^{23–25,39} This model protein system also affords simple kinetics; i.e., no back reactions are expected due to the well-known strong association of biotin and avidin.^{73–75}

Figure 3, top, shows the fluorescein emission intensity from both the silvered and glass (control sample) slide. The emission spectra, which is collected through a 500-nm long-pass filter, shows a ~6-fold greater intensity from the silver as compared to the glass control. As discussed in the introduction, this increase is due to a radiative rate modification of the fluorescein as it is brought into proximity to the silver nanostructures by the bioaffinity reaction and is consistent with numerous publications from our laboratories on the MEF phenomenon.^{19–21,24–39} In Figure 3, top, the sample was incubated for 30 min at room temperature, which was predetermined to be sufficient enough time to allow the assay to go to >95% completion. Figure 3, bottom, shows the normalized spectra, demonstrating that the spectral properties are preserved on both the silver and glass substrates.

Figure 4, top, shows the combined effect of both low-power microwave heating and optical amplification due to the silver^{19–39} for an identical assay as measured in Figure 3, i.e., microwave-accelerated MEF. Interestingly, the assay yields a similar final fluorescence intensity after 20-s microwave heating (~200 au) as compared to a 30-min room-temperature incubation, cf. Figures 3 and 4 top. In addition, the silver still maintains its properties for optically enhancing the fluorescein emission, due to an intrinsic radiative rate modification.^{24,25,39} Figure 4, bottom, shows that the properties of fluorescein are maintained when the spectra are normalized for comparison.

We additionally incubated the assays on both glass and silver for 30 s at room temperature, but with no microwave heating, Figure 5. As we can see, very little fluorescein-labeled avidin was bound to the biotinylated BSA surface, and when compared to the emission intensities shown in Figure 4, then this clearly demonstrates the use of low-power microwaves to increase the rapidity of the assay. This comparison is also evident visually, Figure 6, the photographs on the left taken through an emission filter after 30-s incubation and with no microwave heating, as compared to the right-hand side photographs, which show the much stronger fluorescence emission after 30-s microwave heat-

(64) Petrali, J. P.; Mills K. R. *Microanalysis* **1998**, 114–115.

(65) Link, S.; El-Sayed, M. A. *J. Phys. Chem. B* **1999**, *103*, 8410–8426.

(66) Kreibitz, U.; Genzel, L. *Surf. Sci.* **1985**, *156*, 678–700.

(67) Gao, F.; Lu, Q.; Komarneni, S. *Chem. Mater.* **2005**, *17* (4), 856–860.

(68) Liu, F.-K.; Chang, Y.-C.; Huang, P.-W.; Ko, F.-H.; Chu, T.-C. *Chem. Lett.* **2004**, *33* (8), 1050–1051.

(69) Liu, F.-K.; Huang, P.-W.; Chu, T.-C.; Ko, F.-H. *Mater. Lett.* **2005**, *59* (8–9), 940–944.

(70) Liu, F.-K.; Huang, P.-W.; Chang, Y.-C.; Ko, C.-J.; Ko, F.-H.; Chu, T.-C. *J. Cryst. Growth* **2005**, *273* (3–4), 439–445.

(71) Liu, F.-K.; Huang, P.-W.; Chang, Y.-C.; Ko, F.-H.; Chu, T.-C. *J. Mater. Res.* **2004**, *19* (2), 469–473.

(72) Aslan, K.; Leonenko, Z.; Lakowicz, J. R.; Geddes, C. D. *J. Fluoresc.* **2005**, *15* (5), 643–654.

(73) Green, N. M. *Adv. Protein Chem.* **1975**, *29*, 85–133.

(74) Wilchek, M.; Bayer, E. A. *Anal. Biochem.* **1998**, *171*, 1–6.

(75) Wilchek, M.; Bayer, E. A. *Methods of Enzymology*; Academic Press: San Diego, 1990; Vol. 184.

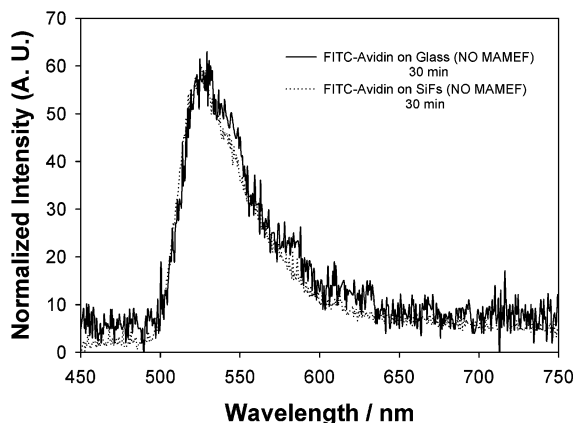
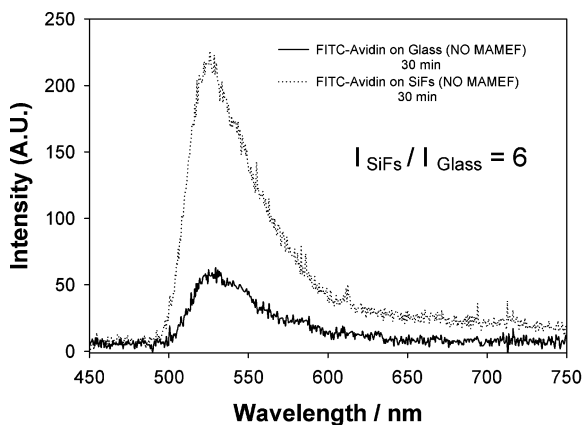


Figure 3. (Top) Enhanced fluorescein emission from the silvered surface as compared to the glass surface (control sample) after 30-min incubation. The samples were washed after incubation. (Bottom) Normalized emission spectra showing that the emission spectral properties are preserved on both silvered and glass substrates.

ing. The top photographs show the microscope slides, the silvered regions appearing brown in color and on the right-hand portion of each slide.

Hence, Figures 4–6 demonstrate the use of low-power microwaves to rapidly heat samples and, when combined with the use of silver nanostructures, readily affords for ultrabright and ultrafast assays. Interestingly, the microwaves do not perturb silver nanostructure morphology or even cause arcing, a familiar characteristic of metallic objects in microwave cavities.⁶⁰ Subsequently, this approach fundamentally addresses two underlying physical constraints of modern assays and immunoassays, namely, assay sensitivity and rapidity. In this regard, the use of the SiFs provides for a ~ 10 -fold increase in signal, which can be translated to increased 10-fold assay sensitivity, while the use of microwaves to facilitate mass protein transport to the surface provides for a ~ 90 -fold decrease in assay run time.

A closer inspection and comparison of Figures 3 and 4, top, reveals that the rapidity of the assay is not equal on both the glass and silver substrates. After 30-min incubation (Figure 3, top) the assay has a maximum emission intensity of ~ 60 au at 530 nm. In comparison, after 20-s microwave heating (Figure 4, top), the emission intensity on the glass control has a value of ~ 25 au. While this decrease lends itself to a larger enhancement ratio observed after microwave heating, i.e., 6 versus 9, we believe that this effect is due to the preferential local heating around the silver nanostructures,⁶⁰ rapidly accelerating mass transport to the

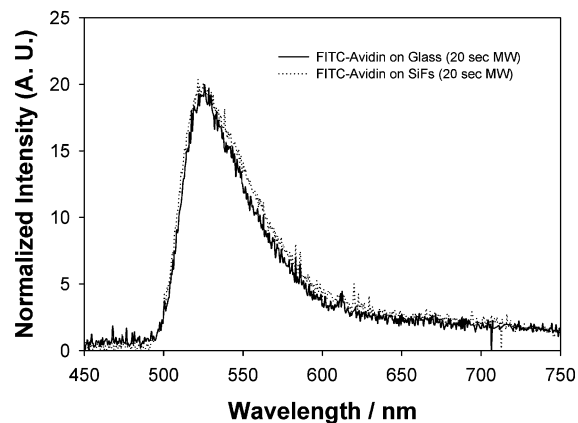
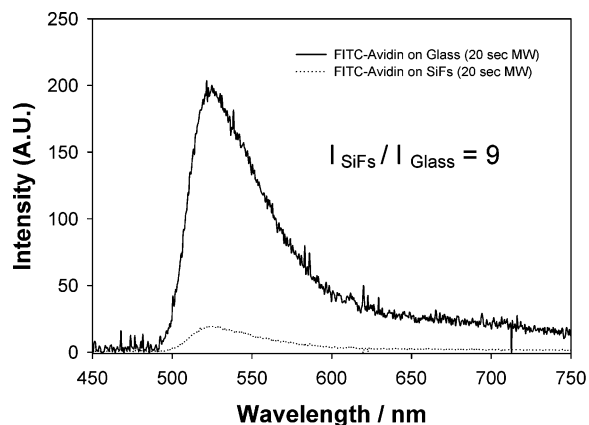


Figure 4. (Top) Enhanced fluorescein emission on the silvered surface as compared to glass after 20-s low-power microwave heating. The sample was washed after 20-s microwaving to remove unbound material. A similar final fluorescein emission fluorescence intensity can be seen for both a 30-min incubation (Figure 3, top) and a 20-s microwave heating. (Bottom) Normalized emission spectra showing that the spectral properties are maintained.

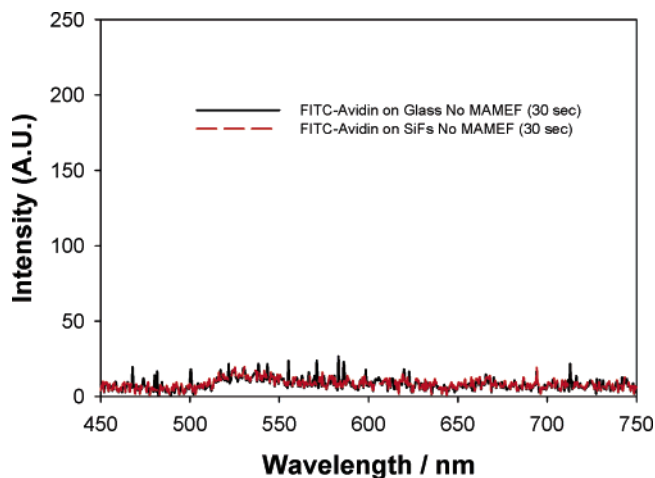


Figure 5. Emission spectra of fluorescein–avidin on both silvered and glass surfaces after 30-s incubation, no microwave heating. The benefits of microwave-accelerated metal-enhanced fluorescence can be seen by comparing Figures 3–5.

surface. Our temperature studies of the assays have shown that, under the conditions employed, only an ~ 8 °C temperature jump occurred (see Temperature Calibration in the Microwave Cavity), which does not account for the 90-fold increase in assay rapidity, further supporting the notion of localized heating. In this regard,

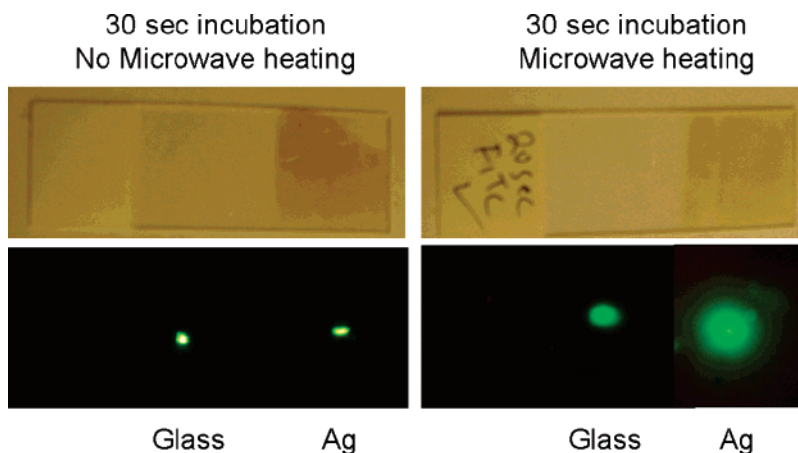


Figure 6. Photographs showing the benefits of MAMEF. Significantly greater fluorescein fluorescence emission intensity can be seen on the silvered surface that has been microwave heated.

Whittaker and Mingos⁶⁰ have indeed reported that metal powders and particles can couple with microwave fields at 2.45 GHz and heat up to temperatures in excess of 1000 °C in very short periods of time, without causing visible electric discharges.⁶⁰ Subsequently, metal powders have been used to accelerate the synthesis of a wide range of metal chalcogenides and as reducing agents in the formation of low-oxidation-state metal cluster compounds.⁶⁰ Although it is likely that there may be contributions from additional plasma effects,⁷⁶ it is believed that the heating of metallic particles and powders by microwaves results primarily from conductive mechanisms.⁶⁰ Attenuation of the microwave radiation in a conductive medium arises from the creation of currents resulting from the charge carriers being displaced in the electric field. The charge carriers are subject to resistance, collisions with lattice phonons,⁶⁰ which lead to ohmic heating.⁶⁰ In our assay, this is thought to lead to the localized heating around the silver particles and is thought to explain the differences in assay rapidity on both the silver and glass substrates.

As briefly described in the introduction, a fluorophore radiative decay rate modification can be characterized by an increased quantum yield (increased fluorescence intensity) coupled with a decreased lifetime, cf. eqs 1 and 2. Subsequently, we measured the fluorescein lifetime from the assay on both the glass and silvered portions after 30-min incubation, as well as after 30-s microwave heating, Figure 7. Remarkably, the intensity decay curves for fluorescein after 30-min incubation as compared to 30-s low-power microwave heating were almost identical, both revealing significantly reduced lifetimes as compared to the glass control. Interestingly, the glass control shows ~80 counts of background, which is due to the longer data acquisition times, a function of the lower S/N of fluorescein on glass as compared to silver. Given the now widespread use of fluorescence spectroscopy for protein structural and environmental information due to the sensitivity of fluorophores to their environment,⁴² we can conclude from Figure 7 that the assays are identical (both conformationally and environmentally), after both a 30-min room temperature incubation and a 30-s microwave heating. These intensity decay curves serve to confirm not only a modification in the fluorophore radiative decay rate, τ_m , but indeed the feasibility of the MAMEF assay

platform. We also later demonstrate that the assay does not undergo any protein conformational changes due to low-power microwave heating, as evidenced by resonance energy-transfer studies; see Effects of Microwave Heating on Protein Conformation.

Fluorophore or analyte photostability is a primary concern in many applications of fluorescence, particularly platform-type assays and single-molecule studies.^{42,77} The maximum number of photons that are emitted by a fluorophore per second is roughly limited by its excited-state lifetime.⁴² Hence, for shorter lifetimes, we can typically observe many more photons per fluorophore per second. This increased photon flux, which lends itself to much improved S/N ratios for assays and therefore improved detectability of analytes, manifests itself as the integrated area under the emission intensity curves of Figures 3 and 4. Clearly, many more photons are emitted per fluorescein molecule in proximity to silver. In addition to an increased detectability, a reduced lifetime in the presence of silver affords for a greater fluorophore photostability, as fluorophores inherently spend less time in an excited state (reduced lifetime) and are therefore less prone to photooxidation, the major photodestruction pathway for fluorescent probes.⁴² Subsequently, we studied the photostability of the fluorescein-based assay after microwave heating to assess any degree of photodestruction, where the assay was first incubated for 30 min at room temperature. Figure 8 shows the cumulative microwave heating of the assay, where the assay was heated and then the fluorescence intensity at 530 nm measured after 470-nm, ~30-mW excitation for 1 min, and the procedure then repeated. After 20-s microwave heating, no change in fluorescein emission was evident on both the glass and silvered slides. In addition, no change in emission signal intensity was evident during the 1-min exposure to laser light, consistent with other reports of enhanced fluorophore photostability by our laboratories.^{19–21} Interestingly, while not shown in Figure 8, under the conditions employed with this assay, it took greater than 3-min microwave heating to dry the assay, up until which point, both the fluorescein emission spectra and peak intensity remained constant.

(76) Baziard Y.; Breton, S.; Toutain, S.; Gourdenne, A. *Eur. Polym. J.* **1988**, *24*, 521–526.

(77) Axelrod, D.; Hellen, E. H. and Fulbright, R. M. Total internal reflection fluorescence. In *Topics in Fluorescence Spectroscopy*, Vol. 3: *Biochemical applications*; Lakowicz, J. R., Ed.; Plenum Press: New York, 1992; pp 289–343.

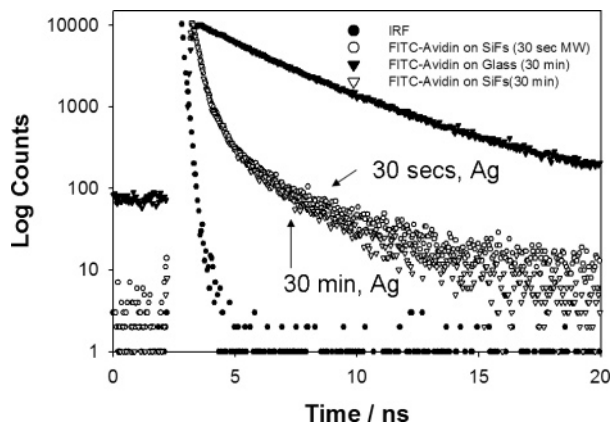


Figure 7. Intensity decays for FITC-avidin on both glass and SiFs, both before and after exposure to low-power microwave heating. The intensity decays on the SiFs are almost identical. IRF, instrument response function.

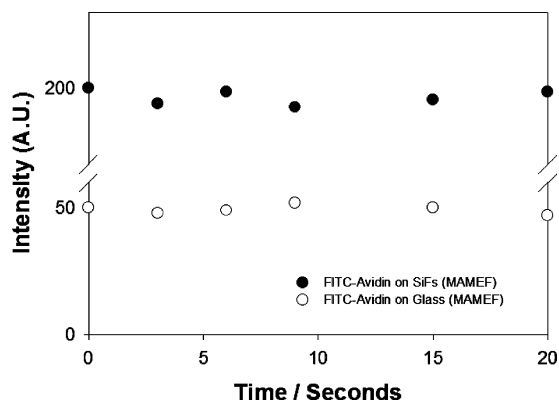


Figure 8. Fluorescein emission intensity from both silvered and glass substrates as a function of cumulative low-power microwave heating. The fluorophore is unperturbed by the microwaves.

Nonspecific Surface Absorption. As with most assays, it is the bioactivity of the species and nature of the surfaces that govern the extent of nonspecific reactions or nonspecific surface assay absorption.^{1–8} Subsequently, we questioned whether the use of low-power microwave heating would indeed increase the rate of nonspecific absorption in our model assay.

We undertook control experiments where both glass and silvered surfaces were incubated with fluorescein-labeled avidin. In these experiments, the surfaces were not precoated with biotinylated BSA. We were able to observe that after 30-min incubation with no microwave heating, essentially no fluorescein was evident from the bare surfaces. This indicates that there is no nonspecific absorption of fluorescein-labeled avidin with the surface. However, after 30-s low-power exposure to microwaves, a very small amount of fluorescein emission was evident on the SiFs. This amount was substantially lower than the >200 au fluorescence intensity shown in Figure 4, top, and is therefore not thought to be of any significance. Subsequently, in our model system, the extent of nonspecific absorption due to microwave heating was deemed negligible.

Effects of Microwave Heating on Protein Conformation.

As briefly mentioned in the introduction, while there is both considerable work and debate concerning DNA or protein damage upon exposure of organisms to microwaves,^{57–59} we investigated whether exposure to microwaves indeed caused protein denatur-

ation in our model assay system. Protein conformational changes on the surface of a metal-enhanced fluorescence assay could potentially complicate assay kinetics and sensitivity, given that MEF is a through-space and distance-dependent phenomenon.^{22–25,39}

Subsequently, we employed FRET to investigate any protein conformational changes, a technique that is widely used and therefore needs no introduction in this regard.⁴² To investigate this, fluorescein (donor, D) and Alexa 532 (acceptor, A) labeled avidin were incubated on surfaces both separately, together and both before and after microwave heating, Figures 9 and 10. In Figure 9, top, we can see that the emission spectral properties of fluorescein-labeled avidin incubated onto a biotinylated BSA surface both before and after microwave heating remain unchanged. Similarly, the acceptor (Alexa 532) incubated alone on the biotinylated surface shows no change in its emission spectral properties, Figure 9, middle. When both the donor and acceptor were incubated together (30 min) on the surface with a D/A ratio of 10:1, then we can clearly see both the fluorescein emission and the Alexa emission, after sole excitation of the donor, Figure 9, bottom. Interestingly, the emission spectra are identical both before and after microwave heating, suggesting that the surface protein assay has not undergone any conformational changes, where such changes would inevitably alter the FRET pair emission spectra.

In Figure 9, bottom, the emission spectra is dominated by the fluorescein emission, primarily because this is in excess, a 10:1 donor/acceptor surface ratio. We subsequently prepared surfaces where the D/A ratio was 1:1, Figure 10. Similarly to Figure 9, the spectra for donor and acceptor alone are unperturbed by microwave heating. However, when the donor and acceptor are incubated together (30 min), the spectrum is no longer dominated by the donor emission, but instead significant energy transfer can be observed to the acceptor, Figure 10, bottom.

Again, after microwave heating, the spectra are almost identical to those not heated, suggesting that no protein conformational changes occur, by the fact that the extent of energy transfer remains constant, i.e., no D/A spectral changes. This strongly suggests that our approach using low-power microwave heating does not modify surface assay morphology.

Advantages of the MAMEF Sensing Platform. In this paper, we have demonstrated a low-cost and simplistic approach to overcoming some of the classical physical constraints imposed by current assay platforms, namely, assay rapidity and sensitivity.^{1–8} Our new MAMEF approach therefore has several notable advantages including the following:

(a) The fluorescence amplification provided by the silver nanostructures has been shown to be applicable to many fluorophores and therefore wavelengths, from the UV to near-IR.^{24,25,39} Hence, fluorophores currently employed in assays would still be suitable. However, the use of low-quantum-yield fluorophores would lead to much larger fluorescence enhancements (i.e., $1/Q_0$) and could significantly reduce unwanted background emission from fluorophores distal from the silvered assay, recalling that MEF is a close-range (<10 nm) through-space interaction.^{24,25,39}

(b) The metal-enhanced fluorescence phenomenon has been shown by us to provide for increased emission intensities,^{19–21} up to several thousand-fold.^{34,78} This substantially increases

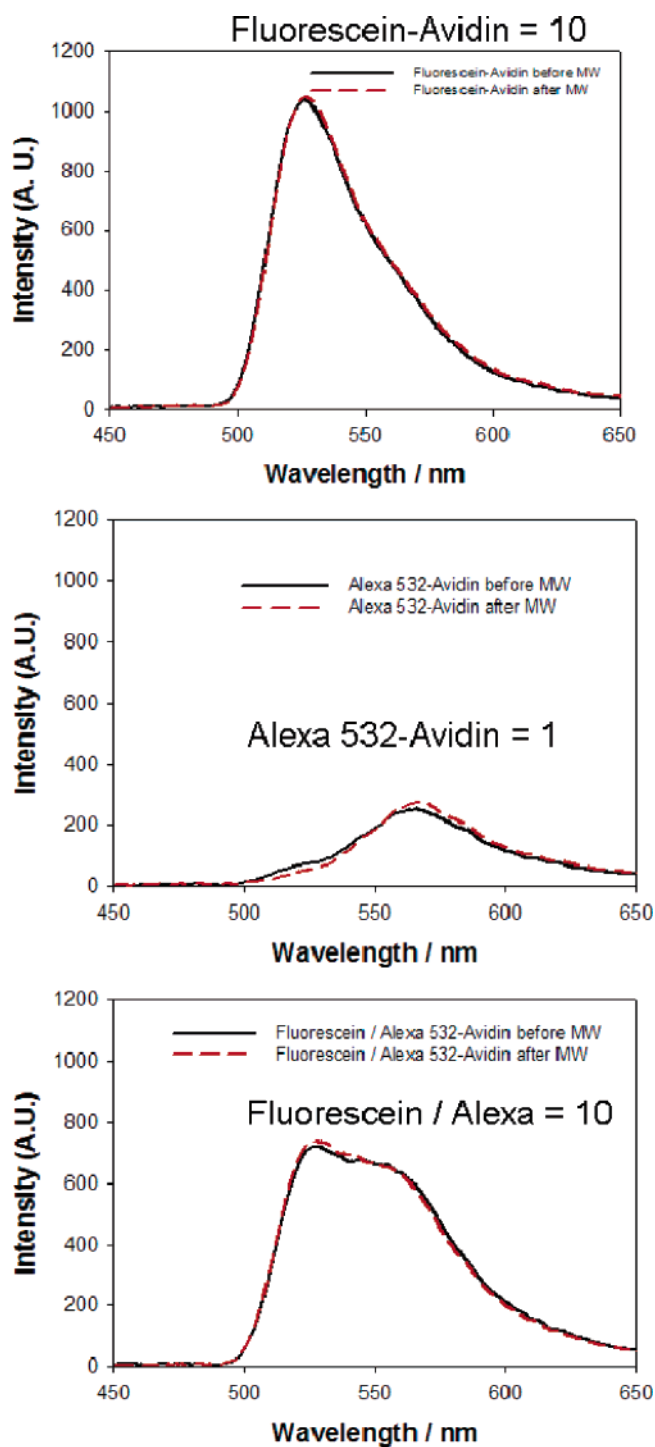


Figure 9. FRET experiments to confirm that the proteins are not denatured by low-power microwaves. (Top) Fluorescein (donor)-labeled avidin before and after low-power microwave heating. (Middle) Alexa 532 (acceptor)-labeled avidin before and after low-power microwave heating. (Bottom) Donor–acceptor-labeled avidin (ratio D/A = 10) before and after low-power microwave heating. The extent of energy transfer does not change after heating, suggesting that the proteins are not denatured.

detection limits (i.e., lower concentrations detectable), which is a major criterion in assay development today.^{1–8}

(c) A whole variety of silvered surfaces can be routinely prepared, which do not require the benefits of a nanofabrication laboratory and sophisticated instrumentation such as electron beam lithography.^{19–21}

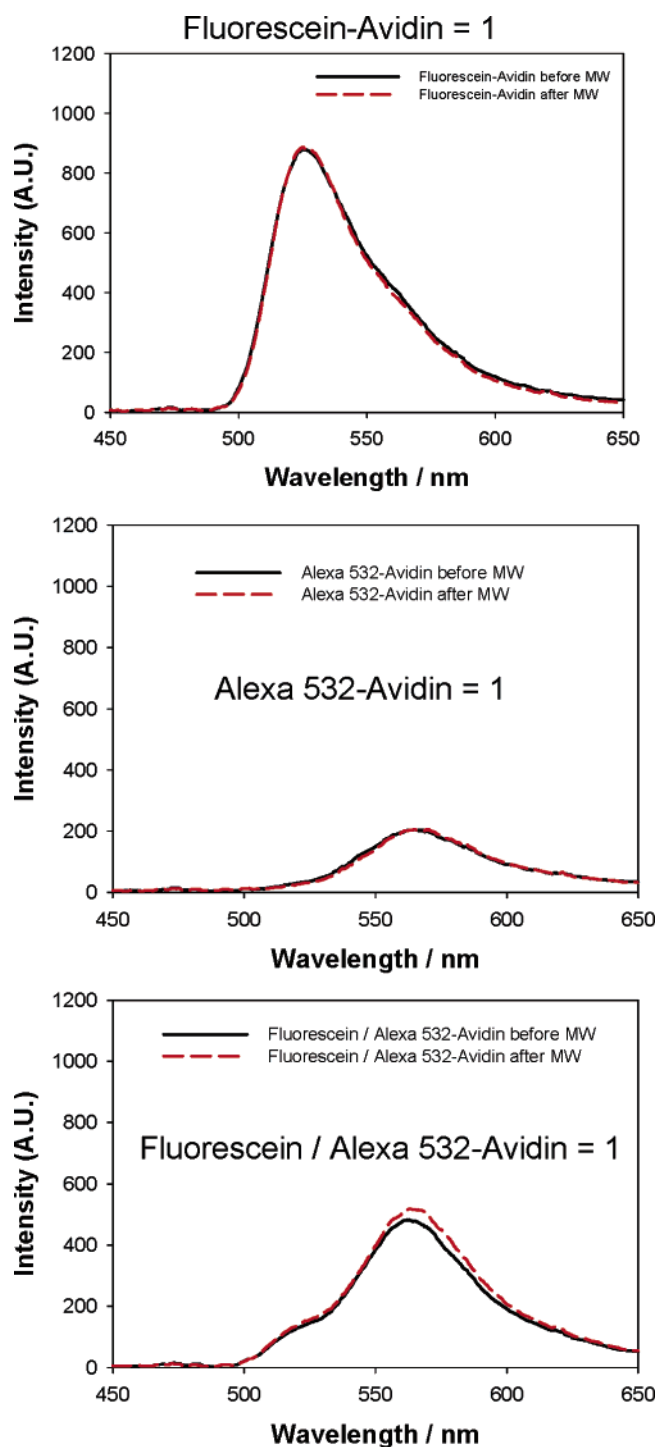


Figure 10. Further FRET experiments to confirm that the proteins are not denatured by low-power microwaves. (Top) Fluorescein (donor)-labeled avidin before and after low-power microwave heating. (Middle) Alexa 532 (acceptor)-labeled avidin before and after low-power microwave heating. (Bottom) Donor–acceptor-labeled avidin (ratio D/A = 1) before and after low-power microwave heating. The extent of energy transfer does not change after heating, suggesting that the proteins are not denatured.

(d) The reduced lifetime of fluorophores in proximity to silver nanostructures provides for a substantially increased fluorophore photostability.^{19–21} In addition, shorter lifetimes allow for higher

(78) Mohamed, M. B.; Volkov, V.; Link, S.; and El-Sayed, M. A., *Chem. Phys. Letts*, **2000**, *317*, 517–523.

fluorophore cycling rates,^{19–21} also providing for increased fluorophore and therefore assay detectability.^{19–21,43}

(e) The low-power microwaves employed here do not perturb the silvered surfaces, do not produce “arcing”, which is commonly observed for metallic objects in microwave cavities,⁶⁰ or even denature or change protein conformation. Low-power microwaves provide for effective rapid heating of the assays, producing identical final fluorescence intensities, fluorophore lifetimes, as well as extents of energy transfer (protein conformation) as compared to room temperature incubation.

CONCLUSIONS

In this paper, we have demonstrated a model assay sensing platform that could be applied to many other fluorescence-based assays currently in use today. This new approach provides for ultrafast and ultrabright assays, an area of immense clinical importance.

The new model assay platform combines the use of silver nanostructures, which can dramatically increase the quantum yield (Γ_m , emissive rate) of proximity fluorophores, with the use of low-power microwaves to rapidly and uniformly heat the assays. The microwaves do not perturb the silver nanostructures or even the assay proteins, but simply increase the mass transport of protein to the silvered surface. For the model assay described here, the use of microwave-accelerated metal-enhanced fluorescence provides for a 10-fold brighter and a 90-fold quicker assay. In immunoassays, such as for the determination of myoglobin levels in the clinical assessment of an acute myocardial infarction, this approach may be of major significance, as current assay times are in excess of 15 min, the sensitivity (100 ng/mL clinical cutoff level⁴³) being determined solely by fluorophore detectability.⁴³

MATERIALS AND METHODS

Materials. Bovine biotinamidocaproyl-labeled albumin (biotinylated BSA), fluorescein (FITC)-labeled avidin, silver nitrate (99.9%), sodium hydroxide (99.996%), ammonium hydroxide (30%), trisodium citrate, D-glucose, and premium quality APS-coated glass slides (75 × 25 mm) were obtained from Sigma-Aldrich. Alexa 532-labeled avidin was obtained from Molecular Probes (Eugene, OR). All chemicals were used as received.

Methods. (1) Formation of Silver Island Films on (3-Aminopropyl)triethoxysilane (APS)-Coated Glass Substrates. In a typical SiF preparation, a solution of silver nitrate (0.5 g in 60 mL of deionized water) in a clean 100-mL glass beaker, equipped with a Teflon-coated stir bar, is prepared and placed on a Corning stirring/hot plate. While stirring at the quickest speed, 8 drops (~200 μ L) of freshly prepared 5% (w/v) sodium hydroxide solution are added. This results in the formation of dark brown precipitates of silver particles. Approximately 2 mL of ammonium hydroxide is then added, drop by drop, to redissolve the precipitates. The clear solution is cooled to 5°C by placing the beaker in an ice bath, followed by soaking the APS-coated glass slides in the solution. While keeping the slides at 5°C, a fresh solution of D-glucose (0.72 g in 15 mL of water) is added. Subsequently, the temperature of the mixture is then warmed to 30 °C. As the color of the mixture turns from yellow-green to yellow-brown, and the color of the slides become green, the slides are removed from the mixture, washed with water, and sonicated for 1 min at room temperature. SiF-deposited slides were then

rinsed with deionized water several times and dried under a stream of nitrogen gas.

SiF-deposited glass slides were then coated with black electrical tape, which is attached to a self-sticking paper, containing three 5-mm-wide circular holes (referred to as a “black body”) on both the silvered and unsilvered slides, prior to the assay fabrication and subsequent fluorescence experiments.

(2) Preparation of the Model Protein Assay (Biotin–Avidin) on Silver Island Films and on Glass (Control Assay).

In previous reports of MEF, our laboratories have coated silvered surfaces with fluorophore-labeled proteins.^{19–21} This experimental format has been adopted for two main reasons, first, that human serum albumin (HSA) is known to bind to silvered surfaces and indeed forms a monolayer,^{73–75} and second, the dimensions of the protein are such that the protein allows for a mean ~4-nm separation of the silver and the fluorophore, MEF being a through-space phenomenon, as demonstrated by the late T. Cotton, our laboratories, and indeed others.^{19–23,79}

The model assay used in this paper is based on the well-known interactions of biotin and avidin. Biotin groups are introduced to the surface through biotinylated BSA, which, similar to HSA, readily forms a monolayer on the surfaces of glass and SiFs.^{73–75} Binding the biotinylated BSA to the SiFs and the glass was accomplished by incubating 10 μ M biotinylated BSA solution in the black body microcuvettes for 1 h, followed by rinsing with water to remove the unbound material. For the model assay, 30 μ L of 1 μ M FITC-labeled avidin was subsequently added into the biotinylated BSA-coated glass and SiF-coated micro-cuvettes, 30 min for the control experiments at room temperature (20 °C), and 20 s in the microwave cavity (0.7 cu ft, GE compact microwave model JES735BF, maximum power 700 W). The power setting was set to 2, which corresponded to 140 W over the entire cavity. This power is similar to the numerous reports using low-power microwaves for immunolabeling,⁸⁰ immunostaining,^{63,64} in immunocytochemistry,^{81–83} and histological microwave processing.^{84,85} In all the experiments performed with low-power microwaves, using both glass slides and quartz cuvettes modified with the black body, there was no evidence of surface drying.

(3) Photostability Experiments. The effect of microwaves on the photostability of FITC was studied by exposing the model assay, which was previously allowed to run to completion at room temperature for 30 min, to microwaves for a cumulative total of 20 s. Approximately 30-mW, 470-nm laser line excitation for 1 min was used before the emission intensity was noted.

(4) FRET Experiments. FRET experiments⁴² were undertaken to evaluate the effect of microwaves on protein conformation and thus denaturation. FITC and Alexa 532 were chosen as the donor–acceptor pair. Two different FITC to Alexa 532 ratios were studied on biotinylated BSA-coated glass slides that were covered with the same black body that was described above. The 10:1 and

(79) Sokolov, K.; Chumanov, G.; Cotton, T. M. *Anal. Chem.* **1998**, *70*, 3898–3905.

(80) Chicoine, L.; Webster, P. *Micro Res. Technol.* **1998**, *42*, 24–32.

(81) Madden, V. J. *Microanalysis* **1998**, *4*, 854–855.

(82) Rangell, L. K.; Keller, G. A. J. *Histochem. Cytochem.* **2000**, *28*, 1153–1160.

(83) Schichnes, D.; Nemson, J.; Sohlberg, L.; Ruzin, S. E. *Microanalysis* **1999**, *4*, 491–496.

(84) Ressner, U. A.; Crumrine, O. A.; Nau, P.; Elias, P. M. *Histochem. J.* **1997**, *29*, 387–392.

(85) Schray, C. L.; Metz, A. L.; Gough, A. W. *Histologic* **2002**, *35* (1), 7–12.

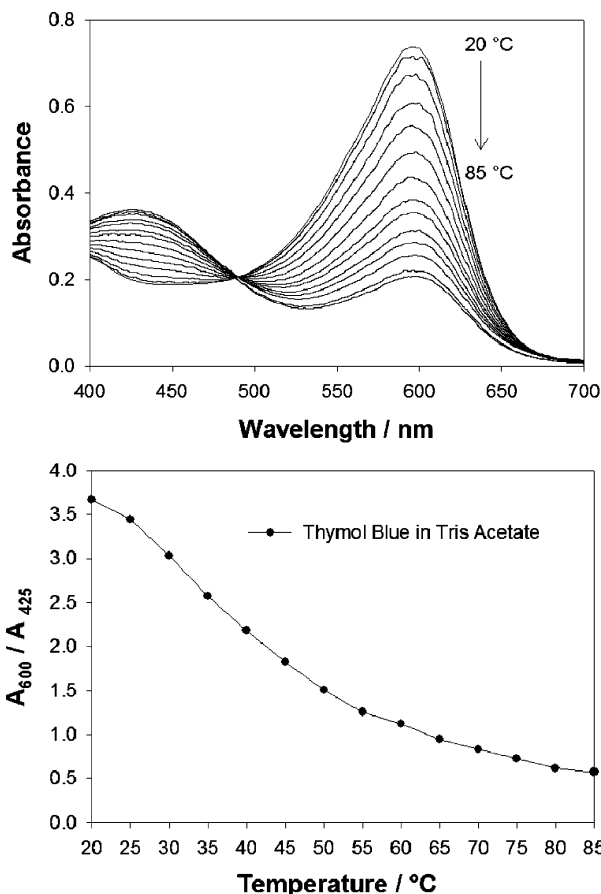


Figure 11. Thymol Blue absorption spectra as a function of temperature (top) and the subsequent ratiometric plot of the 600- and 425-nm absorption bands as a function of temperature (bottom).

1:1 dilutions of FITC–avidin (1 μ M) and Alexa 532–avidin (1 μ M) were incubated on biotinylated BSA-coated glass slides, which were then exposed to microwaves (power setting 2) for 20 s. Fluorescence spectra from the samples, both before and after microwave exposure, were taken.

(5) Absorption, Steady-State, and Time-Resolved Fluorescence Spectroscopy. All absorption measurements were performed using a Varian Cary 50 UV–visible spectrophotometer. Temperature-dependent absorption measurements were performed using a Cary Single Cell Peltier accessory. Fluorescence measurements on SiFs were performed by placing the films on a stationary stage equipped with a fiber-optic mount on a 15-cm-long arm (normal to sample). The output of the fiber was connected to an Ocean Optics HD2000 spectrofluorometer to measure the fluorescence emission spectra. The excitation was from the second harmonic (470 nm) of the diode-pumped Nd:YVO₄ laser (compact laser pointer design, output power \sim 30 mW) at an angle of 45°. The emission was observed through a 500-nm long-pass filter (Edmund Scientific).

Time-resolved intensity decays were measured using reverse start–stop time-correlated single-photon counting⁴² with a Becker and Hickl gmbh 630 SPC PC card and an unamplified MCP–PMT. Vertically polarized excitation at \gg 440 nm was obtained using a pulsed laser diode, 1-MHz repetition rate.

(6) AFM and Real-Color Photographs. AFM images of SiFs were collected using an atomic force microscope (TMX 2100 Explorer SPM, Veeco) equipped with an AFM dry scanner (the

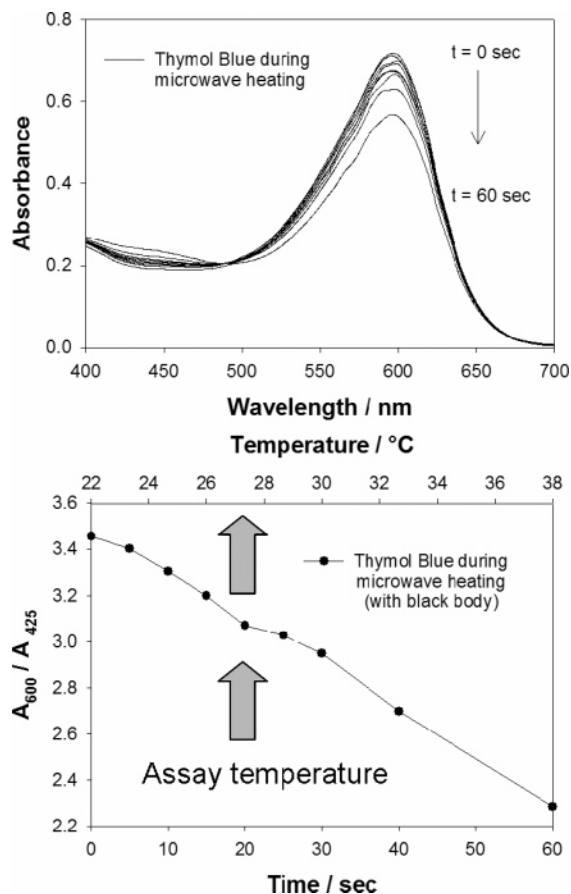


Figure 12. Absorption spectra as a function of temperature for 30 mL Thymol Blue in the black body sample holder (top) and the respective absorbance, temperature vs time ratiometric plot (bottom). The 20 s of microwave heating roughly corresponded to a 8–10 °C temperature jump.

scanning area was 100 \times 100 mm). Surfaces were imaged in air, in a tapping mode of operation, using SFM noncontact mode cantilevers (Veeco). The AFM scanner was calibrated using a standard calibration grid as well as by using gold nanoparticles, 100 nm in diameter from Ted Pella. Images were analyzed using SPMLab software.

The real-color photographs of fluorophore-labeled BSA on SiFs were taken with an Olympus Digital camera (C-740, 3.2 Mega Pixel, 10 \times Optical Zoom) through the same long-pass filter that was used for the emission spectra.

(7) Temperature Calibration in the Microwave Cavity. To calibrate the temperature change during low-power microwave heating, a simple pH thermo-indicator system was used (0.5 mM Thymol Blue, in 50 mM Tris acetate, pH 9.0). In this regard, 30 μ L of a solution of Thymol Blue was placed in a quartz cuvette that was covered with the black body, except for two parallel sides to allow the passage of light for absorption measurements. This arrangement was very similar to that employed on the glass and silvered assay slides. The absorption spectra of the sample were recorded as the temperature was gradually increased from 20 to 85 °C, Figure 11. The color of the solution changed with temperature from deep magenta to pale yellow, due to the temperature dependence of the ionization constant of the Tris buffer. As the temperature was increased, the pH of the solution decreased and the distribution of the ionization states of the

thymol Blue dye changed, resulting in a color change as a function of temperature. The reversible color change is readily observed in the UV–visible spectrum via changes in the 425- and 600-nm spectral bands, Figure 11, top.

The calibration curve (A_{600}/A_{425} vs temperature), Figure 11, bottom, obtained from the above-mentioned calibration measurements, was used to determine the temperature of the sample during the microwave process: the absorption spectra of 30 μL of Thymol Blue in a quartz cuvette covered with the same black body was recorded both before and after microwave heating for up to 60 s, Figure 12, top, where the both the volume used and the black body were the same as actually used in the assays. The ratiometric response (A_{600}/A_{425}) obtained from these samples, Figure 12, bottom, was used to determine the temperature of the sample during microwave heating from the calibration curve. From our calibration plots, a 20-s, 140-W, 2450-MHz microwave exposure resulted in a temperature jump of ~ 8 °C (to ~ 28 °C) for 30 μL of sample. Hence, with this calibration curve, we are simply able to change the assay surface temperature.

It should be noted that a commercially available instrument (such as the Biowave), which is also based on low-power microwaves but uses a thermocouple temperature probe, is available from Ted Pella. This instrument, while inevitably less time-consuming with respect to the needed calibration steps undertaken here, is substantially more costly than the simple approach undertaken in this paper.

(8) Using a Black Body for Assay Temperature Control.

To achieve microwave power tunability and therefore assay temperature and completion time flexibility, we employed black electrical tape to construct small microcuvettes, which held ~ 30 μL of fluid on the surface of both the bare and silvered glass, a volume typically used in high-throughput assays.^{1–8} We found that the presence of the black body had the desirable effect of substantially reducing the local cavity power, where without the black body microcuvettes, 30 μL of surface fluid quickly boiled and dried at 140 W. In essence, the use of the black-bodied microcuvettes, afforded us cavity power tunability between the number 1 and 2 settings on the microwave device, alleviating the need for spending large monies on a tunable commercial instrument.

ACKNOWLEDGMENT

This work was supported by the NIH GM070929 and the National Center for Research Resources, RR008119. Partial salary support to C.D.G. from UMBI is also acknowledged.

Received for review September 8, 2005. Accepted October 19, 2005.

AC0516077